J. Mex. Chem. Soc. **2025**, *69*(4)
Regular Issue

ISSN-e 2594-0317

Impact of the Chemical Speciation of the Ag^{+}–Cl^{-}–e^{-} System on the Construction of True Reference Electrodes and the Potential Purification of the Ionic Liquid 1-Butyl-3-Methylimidazolium Bis(Trifluoromethylsulfonyl)Imide

Jorge Ruvalcaba-Juárez, Oscar Valenzuela-Bonilla, Norma Rodríguez-Laguna, Arturo García-Mendoza*

Sección de Química Analítica, FES Cuautitlán, Universidad Nacional Autónoma de México, Av. Primero de Mayo S/N, Estado de México, 54740, México.

***Corresponding author:** Arturo García-Mendoza, email: arturogm@unam.mx

Received October 9th, 2024; Accepted February 11th, 2025
.

DOI for the article: http://dx.doi.org/10.29356/jmcs.v69i4.2374

Supplementary Information

ISSN-e 2594-0317

Table of contents

Appendix A. Description of the preparation of different REs based on $Ag^0|AgCl_{(s)}$ and $Ag^0|Ag^+$ interfaces in $[C_4mim][NTf_2]$. 4
Fig. S1. Schematic representation of the construction of first-kind (top) and second-kind (bottom) reference electrodes for the $M^0|M^{n+}||$ half-cells in $[C_4mim][NTf_2]$. 4
Table S1. Characteristics and conditions of the internal chamber for the reference electrodes constructed in $[C_4mim][NTf_2]$. 4
Appendix B. Potentiometric calibration curves. 5
Fig. S2. OCP dependence of the Ag^0 and $AgCl_{(s)}$ indicator electrodes as a function of the logarithm of Ag^+ or Cl^- concentration in $[C_4mim][NTf_2]$ at a temperature of 18.8 °C. 5
Fig. S3. OCP dependence of the $AgCl_{(s)}$ indicator electrode as a function of the logarithm of Ag^+ and Cl^- concentration in water at a temperature of 24.6 °C. 5
Table S2. Nernst equations for the $Ag^0|[C_2mim][NTf_2]|$ and $Ag^0|AgCl_{(s)}|[C_2mim][NTf_2]||$ interfaces when employing $Ag[NTf_2]$ solutions; $Ag^0|[C_2mim][NTf_2]||$ and $Ag^0|AgCl_{(s)}|[C_2mim][NTf_2]||$ interfaces when employing $[C_2mim]Cl$ solutions and $Ag^0|AgCl_{(s)}|Cl^-, H_2O||$ interface when employing NaCl solutions. 6
Appendix C. Representative potentiometric titrations and determination of total silver content in $[C_4mim][NTf_2]$. 7
Fig. S4. Records of (A) the evolution of the OCP of an Ag^0 indicator electrode during the titration of $[C_2mim]Cl$ (C_0 = 0.10001 mol L^{-1}) with additions of $Ag[NTf_2]$ (C_{Ag^+} = 0.09972 mol L^{-1}) in $[C_4mim][NTf_2]$ and (B) the corresponding linear fits to the Gran model before the titration endpoint (G(V)) and after it (H(V)). 7
Fig. S5. Records of (A) the evolution of the OCP of an Ag^0 indicator electrode during the titration of $[C_2mim]Cl$ (C_0 = 0.00104 mol L^{-1}) with additions of $Ag[NTf_2]$ (C_{Ag^+} = 0.00099 mol L^{-1}) in $[C_4mim][NTf_2]$ and (B) the corresponding linear fits to the Gran model before the titration endpoint (I(V)) and after it (H(V)). 7
Fig. S6. Records of (A) the evolution of the OCP of an $Ag^0|AgCl_{(s)}$ indicator electrode during the titration of $Ag[NTf_2]$ (C_0 = 0.09972 mol L^{-1}) with additions of $[C_2mim]Cl$ (C_{Cl^-} = 0.10001 mol L^{-1}) in $[C_4mim][NTf_2]$; (B) the corresponding linear fits to the Gran model for J(V) and K(V); and (C) the corresponding linear fits to the Gran model for L(V) and M(V). 8
Fig. S7. Records of (A) the evolution of an $Ag^0|AgCl_{(s)}$ indicator electrode during the titration of Ag^+ remanent in aqueous phase with additions of NaCl (C_{Cl^-} = 0.09930 mol L^{-1}) in aqueous solution and (B) the corresponding linear fits to the Gran model before the titration endpoint (G(V)) and after it (H(V)). 8
Fig. S8. Determination of total silver in an aliquot of $[C_4mim][NTf_2]$ through forming a coordinated silver compound in a buffered medium in an aqueous solution. (A) Records of ASSWV-If for eight additions of a standard solution of $AgNO_3$ in aqueous solution. The parameters used for compound adsorption by chronoamperometry were T = 20.3 °C, t_{pol} = 90 s, and E_{pol} = -0.9 V. The optimized perturbation program for the measurements is as follows: E_{begin} = -0.80 V, E_{end} = 0.25 V, increment in each pulse of 0.002 V, amplitude 0.025 V, and frequency of 120 Hz. The analysis time was 4.8 seconds. All potentials are referenced *vs.* $Ag^0/AgCl_{(s)}$. (B) The calibration curve is based on the standard additions method, showing the dependence of the peak anodic current on the concentration obtained by ASSWV-ΔI. 9
Table S3. Amount of substance, in mmol, for each prepared extraction system determined in both phases. 9
Appendix D. Elucidation of the number of exchanged electrons in the Ag^+–e^- system by chronopotentiometry. 10
Fig. S9. Cyclic voltammograms of the *electrochemical window*. The medium is composed of 3.7182 g of pure $[C_4mim][NTf_2]$ dried in the oven at 90 °C for 24 h. The study was conducted at T = 18 °C under a N_2 atmosphere. Cathodic scan at v = 0.1 V s^{-1}. 10
Fig. S10. (A) Typical chronoamperogram, recorded for a potential pulse of 1.200 V vs. $[Co(Cp)_2]^{+/0}$ for 30 seconds in a solution of $Ag[NTf_2]$, C = 5.95x10^{-4} mol L^{-1}, on a GC electrode. (B) Linear fitting of the Cottrell equation. The measurement was conducted at T = 19 °C with an OCP of 1.366 V vs. $[Co(Cp)_2]^{+/0}$. 11

J. Mex. Chem. Soc. **2025**, *69*(4)
Regular Issue

ISSN-e 2594-0317

Table S4. Diffusion coefficients of Ag^{+} and Cu^{2+} in $[C_4mim][NTf_2]$, estimated by linear fitting of Cottrell's equation. 11
Fig. S11. Linear fit of the Karaoglanoff equation. The measurement was performed at T = 20 °C with an OCP of 1.756 V vs. $[Co(Cp)_2]^{+/0}$. 11
Appendix E. Chemical speciation of the Ag^{+}–Cl^{-}–e^{-} system through the construction of continuous function solubility and extraction diagrams. 12
Fig. S12. (A) Distribution diagram of the predominant chemical species in the system $AgCl_{(s)}/[AgCl_n]^{1-n}$ 13
Table S5. Equations for the construction of theoretical titration curves for $Ag[NTf_2]$ with $[C_2mim]Cl$ and $AgNO_3$ with NaCl under potentiometric monitoring with $Ag^0|AgCl_{(s)}$ and Ag^0 indicator electrodes. 13
Appendix F. Electrochemical behavior of $[Co(Cp)_2]^{+/0}$ in $[C_4mim][NTf_2]$.14
Fig. S13. Typical CV records obtained for the electrolysis of $[Co(Cp)_2]^{+}$ in $[C_4mim][NTf_2]$ using the constructed REs: (A) XF-Type electrode with $Ag^0|AgCl_{(s)}$ interface, (B) XF-Type electrode with $Ag^0|[C_2mim]Cl$ interface, (C) XD-Type electrode with $Ag^0|AgCl_{(s)}$ interface and (D) SH-Type electrode with $Ag^0|Ag^{+}$ interface. The $[Co(Cp)_2](PF_6)$ solutions with an approximate concentration of 25 mmol L^{-1} were stored in a desiccator, and before each measurement, they were bubbled with N_2 for 10 min to remove H_2O. Horizontal arrows indicate the start and direction of the scan. 14
Table S6. Electrochemical parameters for the $[Co(Cp)_2]^{+/0}$ redox couple in $[C_4mim][NTf_2]$, measured by CV, using a three-electrode setup with Au as WE, Pt as CE, and the REs constructed in this work. 14
Appendix G. Electrochemical behavior of $[Fe(Cp)_2CH_2OH)]^{+/0}$ in aqueous solution. 15
Table S7. Electrochemical parameters for the $[Fe(Cp)_2CH_2OH)]^{+/0}$ redox couple in aqueous solution, measured by CV, using a three-electrode setup with Au as WE, Pt as CE, and a commercial reference electrode based on the $Ag^0|AgCl_{(s)}$ interphase. 15

J. Mex. Chem. Soc. **2025**, *69*(4)
Regular Issue

ISSN-e 2594-0317

Appendix A. Description of the preparation of different REs based on $Ag^0|AgCl_{(s)}$ and $Ag^0|Ag^+$ interfaces in $[C_4mim][NTf_2]$.

Four reference electrodes were fabricated: two based on the $Ag^0|AgCl_{(s)}|[C_2mim]Cl$, $[C_4mim][NTf_2]||$ half-cell; one based on the $Ag^0|Ag[NTf_2]$, $[C_4mim][NTf_2]||$ half-cell and one based on the $Ag^0|[C_2mim]Cl$, $[C_4mim][NTf_2]||$ half-cell. These electrodes were constructed in sealed glass tubes using heat-shrink plastic coatings on one side and Vycor® sintered glass stoppers on the other. The wire was soldered to a bronze connection. The Ag^0 and $AgCl_{(s)}$ wires were inserted into the sealed glass tubes with Vycor®, which contained a solution of $[C_2mim]Cl$ or $Ag[NTf_2]$, as sources of Cl^- and Ag^+ as appropriate, prepared in $[C_4mim][NTf_2]$ as is illustrated in Fig. S1. A glass vial containing a small volume of the filling solution for each reference electrode was used as a guard compartment in all the electrodes. The reference electrodes were stored in the dark to avoid photodegradation from UV radiation. The characteristics and labels of each constructed reference electrode are presented in Table S1.

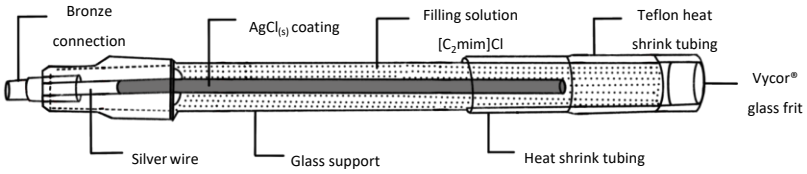

Fig. S1. Schematic representation of the construction of first-kind (top) and second-kind (bottom) reference electrodes for the $M^0|M^{n+}||$ half-cells in $[C_4mim][NTf_2]$.

Table S1. Characteristics and conditions of the internal chamber for the reference electrodes constructed in $[C_4mim][NTf_2]$.

Type[a]	**Interface**	$C_{[C_2mim]Cl}$[b] **/mol L^{-1}**	$C_{Ag[NTf_2]}$[b] **/mol L^{-1}**
XF	$Ag^0\|AgCl_{(s)}\|[C_2mim]Cl$, $[C_4mim][NTf_2]\|\|$	0.01040	–
XF	$Ag^0\|[C_2mim]Cl$, $[C_4mim][NTf_2]\|\|$	0.01040	–
XD	$Ag^0\|AgCl_{(s)}\|[C_2mim]Cl$, $[C_4mim][NTf_2]\|\|$	0.99857	–
SH	$Ag^0\|Ag[NTf_2]$, $[C_4mim][NTf_2]\|\|$	–	0.29936

[a] The annotations used as labels refer to the expected solute concentration in the internal chamber (D for 0.1000 mol L^{-1}, F for 0.0100 mol L^{-1},and H for 0.3000 mol L^{-1}); the type of solute employed (S for $Ag[NTf_2]$, and X for Cl^-).

[b] The molar concentrations were calculated assuming that the density of the $[C_2mim]Cl$ with $[C_4mim][NTf_2]$ mixture and $Ag[NTf_2]$ with $[C_4mim][NTf_2]$ is the same as that of the pure ionic liquid. The values presented correspond to the results of their respective standardizations.

J. Mex. Chem. Soc. **2025**, *69*(4)
Regular Issue

ISSN-e 2594-0317

Appendix B. Potentiometric calibration curves.

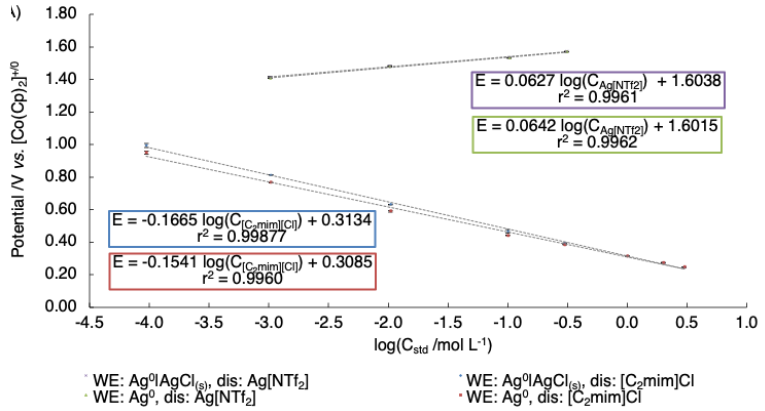

Fig. S2. OCP dependence of the Ag^0 and $AgCl_{(s)}$ indicator electrodes as a function of the logarithm of Ag^+ or Cl^- concentration in $[C_4mim][NTf_2]$ at a temperature of 18.8 °C.

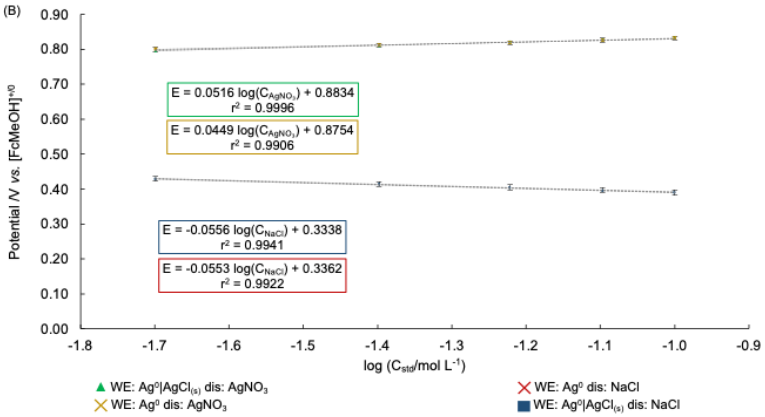

Fig. S3. OCP dependence of the $AgCl_{(s)}$ indicator electrode as a function of the logarithm of Ag^+ and Cl^- concentration in water at a temperature of 24.6 °C.

J. Mex. Chem. Soc. **2025**, *69*(4)
Regular Issue

ISSN-e 2594-0317

Table S2. Nernst equations for the $Ag^0|[C_2mim][NTf_2]|$ and $Ag^0|AgCl_{(s)}|[C_2mim][NTf_2]||$ interfaces when employing $Ag[NTf_2]$ solutions; $Ag^0|[C_2mim][NTf_2]||$ and $Ag^0|AgCl_{(s)}|[C_2mim][NTf_2]||$ interfaces when employing $[C_2mim]Cl$ solutions and $Ag^0|AgCl_{(s)}|Cl^-, H_2O||$ interface when employing NaCl solutions.

Interface	Standard used in RTIL	Representative chemical equilibrium at the interface	Nernst equation
Ag^0	$Ag[NTf_2]$	$Ag^0 \rightleftarrows Ag^+ + e^-$	$E_{RE} = E^{\circ'}_{Ag^+/Ag^0} + \frac{RT\ln(10)}{F}\log\,[Ag^+]$
$Ag^0\|AgCl_{(s)}$	$Ag[NTf_2]$	$Ag^0 + Cl^- \rightleftarrows AgCl_{(s)} + e^-$	$E_{RE} = E^{\circ'}_{AgCl_{(s)}/Ag^+} - \frac{RT\ln(10)}{F}\log K_{sp} + \frac{RT\ln(10)}{F}\log\,[Ag^+]$
Ag^0	$[C_2mim]Cl$	$Ag^0 + 3Cl^- \rightleftarrows [AgCl_3]^{2-} + e^-$	$E_{RE} = E^{\circ''}_{[AgCl_3]^{2-}/Ag^0} - \frac{3RT\ln(10)}{F}\log\,[Cl^-]$
$Ag^0\|AgCl_{(s)}$	$[C_2mim]Cl$	$Ag^0 + 3Cl^- \rightleftarrows [AgCl_3]^{2-} + e^-$	$E_{RE} = E^{\circ''}_{[AgCl_3]^{2-}/Ag^0} - \frac{3RT\ln(10)}{F}\log\,[Cl^-]$
$Ag^0\|AgCl_{(s)}$	NaCl[a]	$Ag^0 + Cl^- \rightleftarrows AgCl_{(s)} + e^-$	$E_{RE} = E^{\circ'}_{AgCl_{(s)}/Ag^0} - \frac{3RT\ln(10)}{F}\log\,[Cl^-]$
$Ag^0\|AgCl_{(s)}$	$AgNO_3$[a]	$Ag^0 \rightleftarrows Ag^+ + e^-$	$E_{RE} = E^{\circ'}_{AgCl_{(s)}/Ag^+} - \frac{RT\ln(10)}{F}\log K_{sp} + \frac{RT\ln(10)}{F}\log\,[Ag^+]$

[a] This standard was prepared in an aqueous solution.

J. Mex. Chem. Soc. **2025**, *69*(4)
Regular Issue

ISSN-e 2594-0317

Appendix C. Representative potentiometric titrations and determination of total silver content in [C_4mim][NTf_2].

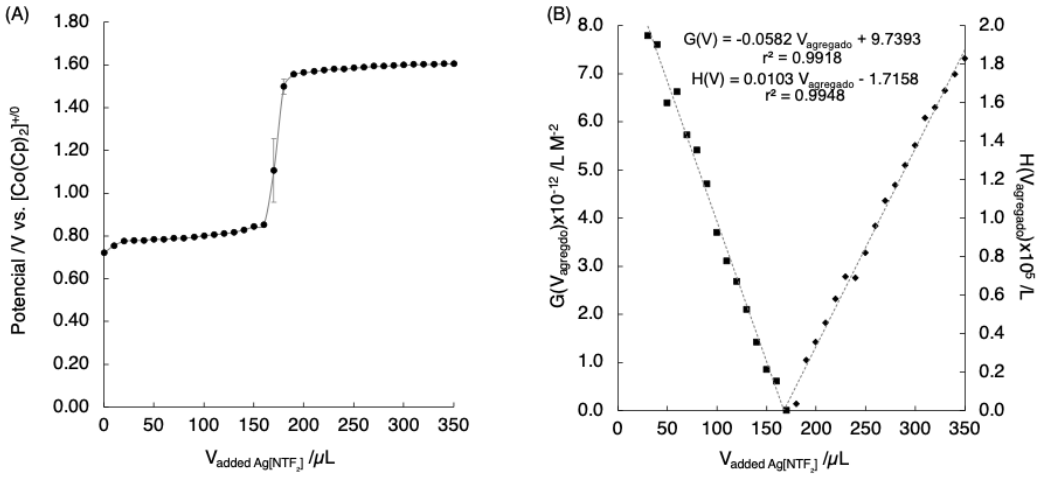

Fig. S4. Records of **(A)** the evolution of the OCP of an Ag^0 indicator electrode during the titration of [C_2mim]Cl (C_0 = 0.10001 mol L^{-1}) with additions of Ag[NTf_2] (C_{Ag^+} = 0.09972 mol L^{-1}) in [C_4mim][NTf_2] and **(B)** the corresponding linear fits to the Gran model before the titration endpoint (G(V)) and after it (H(V)).

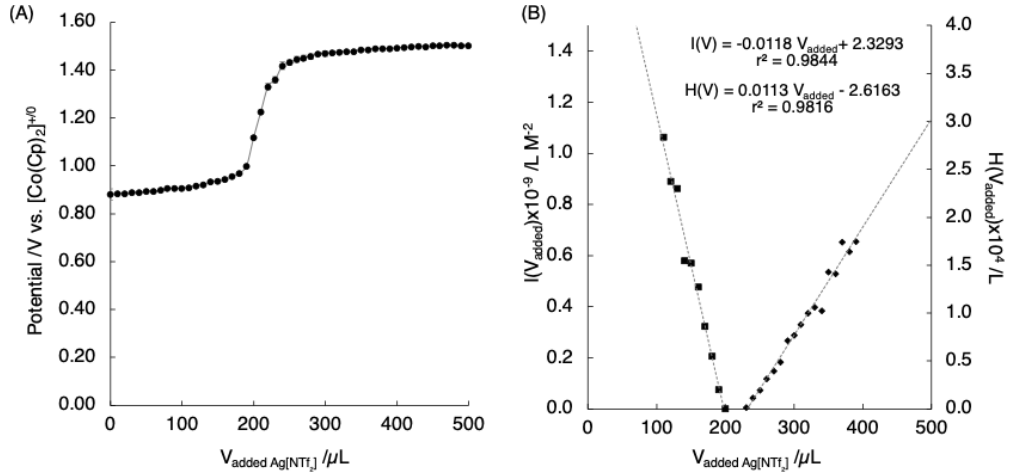

Fig. S5. Records of **(A)** the evolution of the OCP of an Ag^0 indicator electrode during the titration of [C_2mim]Cl (C_0 = 0.00104 mol L^{-1}) with additions of Ag[NTf_2] (C_{Ag^+} = 0.00099 mol L^{-1}) in [C_4mim][NTf_2] and **(B)** the corresponding linear fits to the Gran model before the titration endpoint (I(V)) and after it (H(V)).

J. Mex. Chem. Soc. **2025**, *69*(4)
Regular Issue

ISSN-e 2594-0317

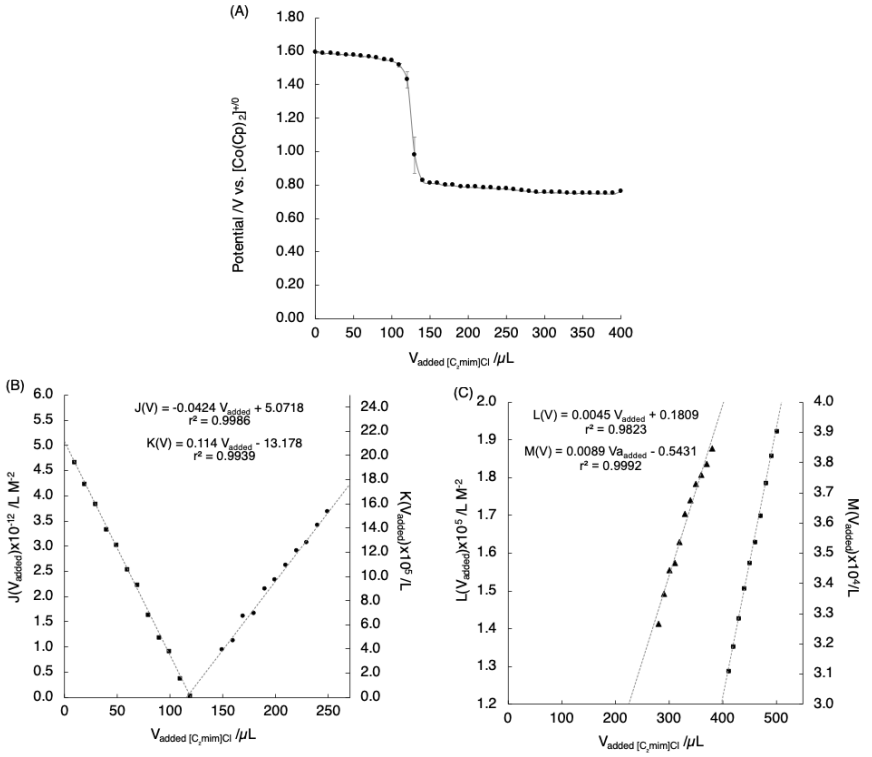

Fig. S6. Records of **(A)** the evolution of the OCP of an $Ag^0|AgCl_{(s)}$ indicator electrode during the titration of $Ag[NTf_2]$ (C_0 = 0.09972 mol L^{-1}) with additions of $[C_2mim]Cl$ (C_{Cl^-} = 0.10001 mol L^{-1}) in $[C_4mim][NTf_2]$; **(B)** the corresponding linear fits to the Gran model for J(V) and K(V); and **(C)** the corresponding linear fits to the Gran model for L(V) and M(V).

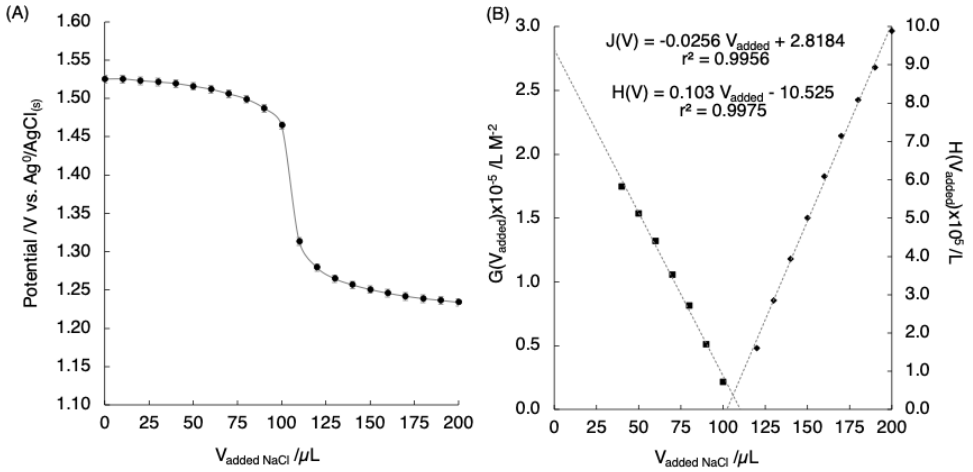

Fig. S7. Records of **(A)** the evolution of an $Ag^0|AgCl_{(s)}$ indicator electrode during the titration of Ag^+ remanent in aqueous phase with additions of NaCl (C_{Cl^-} = 0.09930 mol L^{-1}) in aqueous solution and **(B)** the corresponding linear fits to the Gran model before the titration endpoint (G(V)) and after it (H(V)).

J. Mex. Chem. Soc. **2025**, *69*(4)
Regular Issue

ISSN-e 2594-0317

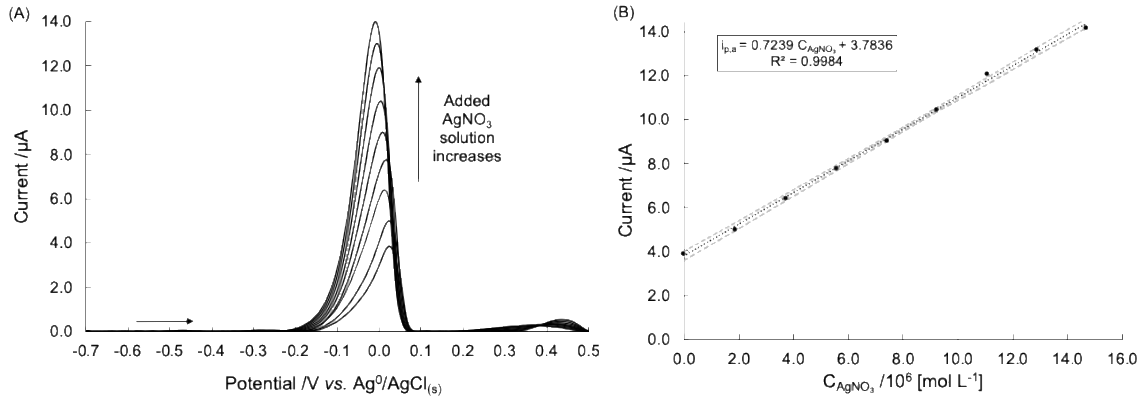

Fig. S8. Determination of total silver in an aliquot of $[C_4mim][NTf_2]$ through forming a coordinated silver compound in a buffered medium in an aqueous solution. **(A)** Records of ASSWV-If for eight additions of a standard solution of $AgNO_3$ in aqueous solution. The parameters used for compound adsorption by chronoamperometry were T = 20.3 °C, t_{pol} = 90 s, and E_{pol} = -0.9 V. The optimized perturbation program for the measurements is as follows: E_{begin} = -0.80 V, E_{end} = 0.25 V, increment in each pulse of 0.002 V, amplitude 0.025 V, and frequency of 120 Hz. The analysis time was 4.8 seconds. All potentials are referenced *vs.* $Ag^0/AgCl_{(s)}$. **(B)** The calibration curve is based on the standard additions method, showing the dependence of the peak anodic current on the concentration obtained by ASSWV-ΔI.

Table S3. Amount of substance, in mmol, for each prepared extraction system determined in both phases.

System	$p(V_{org}/V_{ac})$	pH	Substance in organic phase [mmoL] $x10^{-05}$	Substance in aqueous phase [mmoL] $x10^{-03}$
A	-0.01	3.47	2.67	9.57
B	-0.22	3.47	7.33	9.57
C	0.17	3.47	6.19	9.53
D	0.20	3.47	6.57	9.57
E	0.20	7.86	5.90	7.32
F	0.19	11.49	6.04	6.87
G	0.70	8.64	3.31	5.79

J. Mex. Chem. Soc. **2025**, *69*(4)
Regular Issue

ISSN-e 2594-0317

Appendix D. Elucidation of the number of exchanged electrons in the Ag^{+}–e^{-} system by chronopotentiometry. To determine and ensure the number of exchanged electrons involved in the reaction associated with the Ag^{0}/Ag^{+} redox couple a chronoamperometric study was carried out.

The electrochemical windows (ECW) were obtained by cyclic voltammetry (CV) in a 3-electrode cell using a glassy carbon electrode (GC) as working electrode (WE). The measurements commenced from the open-circuit potential, and the voltammograms of the reaction medium are shown in Fig. S7. The potential inversion points were carefully selected to ensure that the current of the barriers fell between 50 and 100 μA.

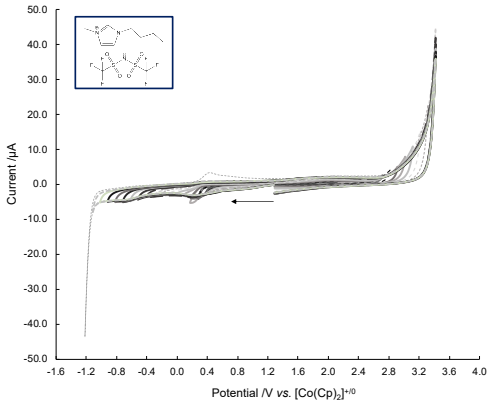

Fig. S9. Cyclic voltammograms of the *electrochemical window*. The medium is composed of 3.7182 g of pure $[C_4mim][NTf_2]$ dried in the oven at 90 °C for 24 h. The study was conducted at T = 18 °C under a N_2 atmosphere. Cathodic scan at v = 0.1 V s^{-1}.

The Sand equation (Equation S1) was used to evaluate the diffusion coefficient of the oxidant or reductant, as applicable, to calculate the electrolysis current. Therefore, chronoamperometric studies were conducted to estimate the diffusion coefficient of Ag^{+} specie quickly and directly, using the Cottrell equation (Equation S2). The chronoamperogram in RTIL media, along with the Cottrell fit, are depicted in Fig. S10.

$$i\tau^{1/2} = \frac{\pi^{1/2} n F A D_i^{1/2} C_i^*}{2} \qquad \text{Equation S1}$$

$$i(t) = i_d(t) = \frac{n F A D_O^{1/2} C_0^*}{\pi^{1/2} t^{1/2}} \qquad \text{Equation S2}$$

J. Mex. Chem. Soc. **2025**, *69*(4)
Regular Issue

ISSN-e 2594-0317

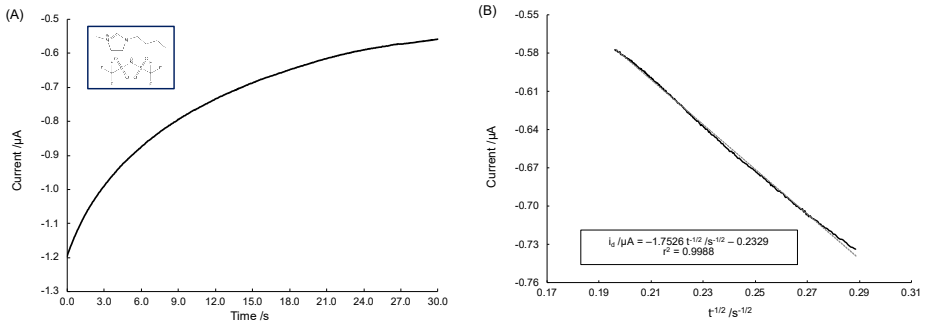

Fig. S10. (A) Typical chronoamperogram, recorded for a potential pulse of 1.200 V vs. $[Co(Cp)_2]^{+/0}$ for 30 seconds in a solution of $Ag[NTf_2]$, C = 5.95x10^{-4} mol L^{-1}, on a GC electrode. **(B)** Linear fitting of the Cottrell equation. The measurement was conducted at T = 19 °C with an OCP of 1.366 V vs. $[Co(Cp)_2]^{+/0}$.
The diffusion coefficient found in each solvent are reported in Table S4.

Table S4. Diffusion coefficients of Ag^+ and Cu^{2+} in $[C_4mim][NTf_2]$, estimated by linear fitting of Cottrell's equation.

Specie	D_O /cm^2 s^{-1}
Ag^+	7.54x10^{-7}

In Fig. S11 the linear Karaoglanoff fit is presented for the chronopotentiogram obtained in $[C_4mim][NTf_2]$. It was found that the value of $E_{\tau/4}$ vs. $[Co(Cp)_2]^{+/0}$ for the $Ag^{+/0}$ redox couple was 1.8904 V, and the number of electrons exchanged in the semi-reaction corresponds to 1.01. This value guarantees that the $Ag^{+/0}$ redox couple exchanges one and only one electron in the semi-reaction. The transition time, τ, for the linear fit was 27 seconds, and it was short enough to avoid adsorption processes and IL contamination due to water absorption.

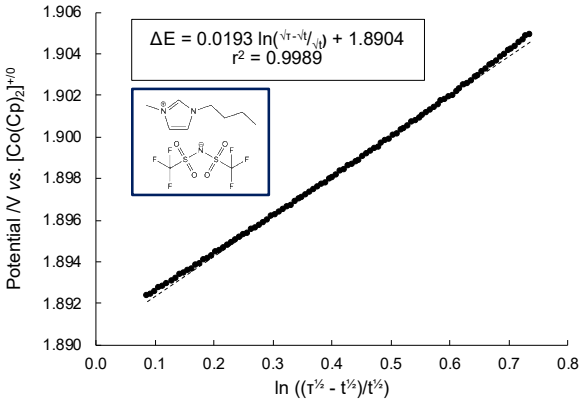

Fig. S11. Linear fit of the Karaoglanoff equation. The measurement was performed at T = 20 °C with an OCP of 1.756 V vs. $[Co(Cp)_2]^{+/0}$.

J. Mex. Chem. Soc. **2025**, *69*(4)
Regular Issue

ISSN-e 2594-0317

Appendix E. Chemical speciation of the Ag^{+}–Cl^{-}–e^{-} system through the construction of continuous function solubility and extraction diagrams.

Distribution diagrams, φ_i, were constructed as a function of pCl, using the Method of Extended Ringbom's Coefficients (MERC), to determine the predominant chemical species in the Ag^{+}–Cl^{-} system. Subsequently, the φ_i functions are presented to construct the distribution diagrams in a homogeneous system, *i.e.*, when $C_0 < S_0$ for silver (Equation S3).

$$\phi_0 = \phi_{Ag^+} = (1 + \beta_1 10^{-pCl} + \beta_2 10^{-2pCl} + \beta_3 10^{-3pCl})^{-1}$$

$$\phi_1 = \phi_{[AgCl]} = \phi_0(\beta_1 10^{-pCl})$$

$$\phi_2 = \phi_{[AgCl_2]^-} = \phi_0(\beta_2 10^{-2pCl}) \qquad \text{Equation S3}$$

$$\phi_3 = \phi_{[AgCl_3]^{2-}} = \phi_0(\beta_3 10^{-3pCl})$$

On the other hand, Equation S4 presents the expressions of $\bar{\varphi}_i$ that describe the distribution of chemical species in a heterogeneous system, consisting of a dispersed phase in contact with a precipitated solid phase for the silver system. The expressions are constructed based on the material balance, where the activity of $AgCl_{(s)}$ specie is rewritten using the solubility equilibrium. Note the incorporation of a term describing the fraction of the insoluble species.

$$\bar{\phi}_0 = \bar{\phi}_{Ag^+} = (1 + \beta_1 10^{-pCl} + \beta_2 10^{-2pCl} + \beta_3 10^{-3pCl} + C_0 \beta_1^{\circ} 10^{-pCl})^{-1}$$

$$\bar{\phi}_1 = \bar{\phi}_{[AgCl]} = \bar{\phi}_0 (\beta_1 10^{-pCl})$$

$$\bar{\phi}_2 = \bar{\phi}_{[AgCl_2]^-} = \bar{\phi}_0 (\beta_2 10^{-2pCl}) \qquad \text{Equation S4}$$

$$\bar{\phi}_3 = \bar{\phi}_{[AgCl_3]^{2-}} = \bar{\phi}_0 (\beta_3 10^{-3pCl})$$

$$\bar{\phi}_{AgCl_{(s)}} = \bar{\phi}_0 (C_0 \bar{\beta}_1 10^{-pCl})$$

The construction of the solubility diagram presented in Fig. 5 was performed following Equation S5, which allows us to describe the transition of the systems between different phases.

$$\log(s'/M) = \log(C_0/M) + \log\left(\frac{\alpha_{M(L)}}{\bar{\alpha}_{M(L)}}\right) \qquad \text{Equation S5}$$

J. Mex. Chem. Soc. **2025**, *69*(4)
Regular Issue

ISSN-e 2594-0317

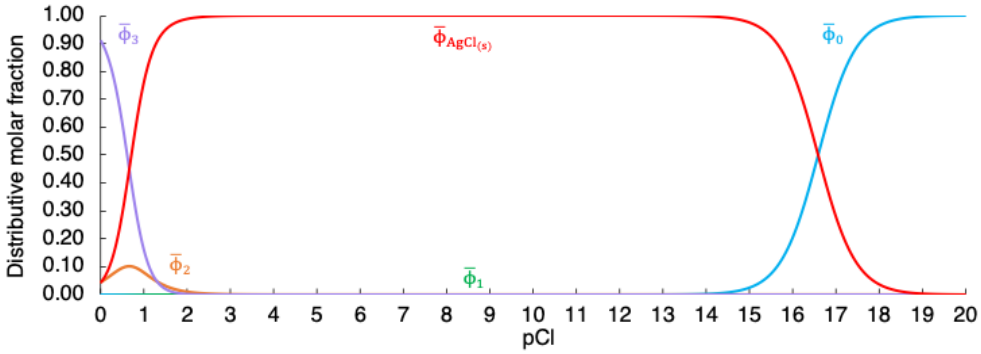

Fig. S12. (A) Distribution diagram of the predominant chemical species in the system $AgCl_{(s)}/[AgCl_n]^{1-n}$

Table S5 presents the equations used to construct the theoretical titration curves for $Ag[NTf_2]$ with $[C_2mim]Cl$ under potentiometric monitoring with an $Ag^0|AgCl_{(s)}$ indicator electrode; $Ag[NTf^2]$ with $[C_2mim]Cl$ using potentiometric monitoring with an Ag^0 indicator electrode; and $AgNO_3$ with NaCl using potentiometric monitoring with an $Ag^0|AgCl_{(s)}$ indicator electrode.

Table S5. Equations for the construction of theoretical titration curves for $Ag[NTf_2]$ with $[C_2mim]Cl$ and $AgNO_3$ with NaCl under potentiometric monitoring with $Ag^0|AgCl_{(s)}$ and Ag^0 indicator electrodes.

Analyte	**Titrant**	**Indicator electrode**	**Solvent**	**Equations for the theoretical curve** [a]
$[C_2mim]Cl$	$Ag[NTf_2]$	$Ag^0\|AgCl_{(s)}$	$[C_4mim][NTf_2]$	$v = \frac{v_0 10^{-pCl} + v_0 C_0(1 - \bar{\varphi}_0 + \bar{\varphi}_2 + 2\bar{\varphi}_3)}{C_T - 10^{-pCl}}$
$[C_2mim]Cl$	$Ag[NTf_2]$	Ag^0 [a]	$[C_4mim][NTf_2]$	$v = \frac{v_0 C_0(\bar{\varphi}_0 + \bar{\varphi}_2 + 2\bar{\varphi}_3 - 1) - v_0 10^{-pAg}}{10^{-pAg} - C_T}$
$AgNO_3$	NaCl	$Ag^0\|AgCl_{(s)}$	H_2O	$v = \frac{v_0 10^{-pCl} + v_0 C_0(1 + \bar{\varphi}_2 + 2\bar{\varphi}_3 + 3\bar{\varphi}_4 - \bar{\varphi}_0)}{C_T - 10^{-pCl}}$

[a] The equations associated with the distributive mole fractions for constructing the theoretical titration curve are not as straightforward as ones used in a common homogeneous titration.

On the other hand, the construction of the conditional extraction diagram for the water-$[C_4mim][NTf_2]$ system as a function of pCl (Fig. 3) was carried out using a non-segmented polynomial, applying Ringbom's coefficients in both phases while considering the chloride species in the aqueous medium and $[C_4mim][NTf_2]$, according to Equation S6.

$$\log K_E' = \log K_E + \log\left(\bar{\alpha}_{Ag(I)(Cl)}\right)_{aq} - \log\left(\bar{\alpha}_{Ag(I)(Cl)}\right)_{RTIL} \qquad \text{Equation S6}$$

J. Mex. Chem. Soc. **2025**, *69*(4)
Regular Issue

ISSN-e 2594-0317

Appendix F. Electrochemical behavior of $[Co(Cp)_2]^{+/0}$ in $[C_4mim][NTf_2]$.

The CV records of $[Co(Cp)_2]^{+/0}$ in $[C_4mim][NTf_2]$ exhibit a profile similar to that obtained in conventional solvents. These records are presented in Fig. S13 at the nine analyzed scan rates.

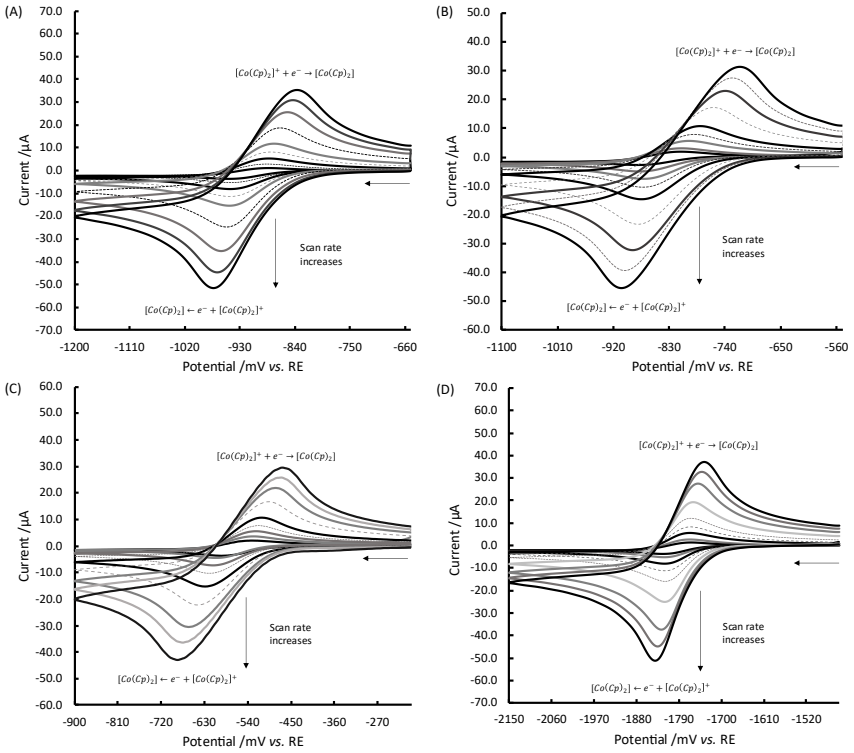

Fig. S13. Typical CV records obtained for the electrolysis of $[Co(Cp)_2]^+$ in $[C_4mim][NTf_2]$ using the constructed REs: (A) XF-Type electrode with $Ag^0|AgCl_{(s)}$ interface, (B) XF-Type electrode with $Ag^0|[C_2mim]Cl$ interface, (C) XD-Type electrode with $Ag^0|AgCl_{(s)}$ interface and (D) SH-Type electrode with $Ag^0|Ag^+$ interface. The $[Co(Cp)_2](PF_6)$ solutions with an approximate concentration of 25 mmol L^{-1} were stored in a desiccator, and before each measurement, they were bubbled with N_2 for 10 min to remove H_2O. Horizontal arrows indicate the start and direction of the scan.

Table S6. Electrochemical parameters for the $[Co(Cp)_2]^{+/0}$ redox couple in $[C_4mim][NTf_2]$, measured by CV, using a three-electrode setup with Au as WE, Pt as CE, and the REs constructed in this work.

Parameter	**RE XF** [b] **$Ag^0|AgCl_{(s)}$**	**Re XF** [b] **$Ag^0|Cl^-$**	**RE XD** [b] **$Ag^0|AgCl_{(s)}$**	**RE SH** [b] **$Ag^0|Ag^+$**
$E°'_{O/R}$/V	-0.963 ± 0.035	-0.989 ± 0.033	-0.571 ± 0.002	-1.780 ± 0.002
D_O /10^{-7} cm^2 s^{-1}	2.210 ± 0.460	1.506 ± 0.038	1.393 ± 0.051	1.491 ± 0.043
D_R /10^{-7} cm^2 s^{-1}	0.960 ± 0.050	1.335 ± 0.042	1.165 ± 0.050	1.238 ± 0.046
D_O/D_R	1.38	1.16	1.22	1.22
$D_O\eta$ /10^{-6} g cm s^{-2}	8.47	9.21	8.52	9.12
k^0 /10^{-3} cm s^{-1}	3.5 ± 1.1	7.2 ± 1.1	0.9 ± 0.2	1.9 ± 0.2
R_s /Ω[a]	1004.6	1135.2	1093.9	1136.7

[a] The solution resistance was determined through compensation for ohmic drop, iR.

J. Mex. Chem. Soc. **2025**, *69*(4)
Regular Issue

ISSN-e 2594-0317

Appendix G. Electrochemical behavior of $[Fe(Cp)_2CH_2OH)]^{+/0}$ in aqueous solution.

The CV records of the electrolysis of $[Fe(Cp)_2CH_2OH)]^{+/0}$ exhibit a typical reversible profile. Electrochemical parameters obtained from these CV measurements are presented in Table S7.

Table S7. Electrochemical parameters for the $[Fe(Cp)_2CH_2OH)]^{+/0}$ redox couple in aqueous solution, measured by CV, using a three-electrode setup with Au as WE, Pt as CE, and a commercial reference electrode based on the $Ag^0|AgCl_{(s)}$ interphase.

Parameter	**RE** **$Ag^0\|AgCl_{(s)}$**
$E°'_{O/R}$/V	0.150 ± 0.003
D_O /10^{-6} cm^2 s^{-1}	4.387 ± 0.030
D_R /10^{-6} cm^2 s^{-1}	5.269 ± 0.023
D_O/D_R	0.83
$D_O\eta$ /10^{-6} g cm s^{-2}	5.27
k^0 /10^{-2} cm s^{-1}	4.7 ± 0.5
R_s /Ω[a]	702.6

[a] The solution resistance was determined through compensation for ohmic drop, iR.